



Cite this: DOI: 10.1039/d6sc00891g

All publication charges for this article have been paid for by the Royal Society of Chemistry

# Electrolyte-anion-controlled reactivity of aromatic radical cations

Naoki Shida,<sup>a</sup> Takuma Maekawa,<sup>d</sup> Yuki Yasuno,<sup>a</sup> Su-Gi Chong,<sup>b</sup> Ikuyoshi Tomita,<sup>d</sup> Mahito Atobe<sup>b</sup> and Shinsuke Inagi<sup>d</sup>

Electrolytes are indispensable in electrosynthesis, yet their function is generally confined to ionic conduction. Here we show that specific association of electrolyte anions provides a powerful means to regulate the reactivity of electrogenerated aromatic radical cations. Electrochemical oxidation of 2,5-diarylthiophenes in the presence of a coordinating anion, triflate (TfO<sup>-</sup>), selectively triggers C–C bond formation, leading to dimerization followed by oxidative cyclization to afford thiophenium cations. In contrast, weakly coordinating anions such as B(C<sub>6</sub>F<sub>5</sub>)<sub>4</sub><sup>-</sup> stabilize persistent and largely unreactive radical cations. Spectroscopic analyses confirm radical cation formation under weakly coordinating conditions, while the presence of a coordinating anion fundamentally alters the reaction pathway, selectively enabling productive C–C bond formation. These results establish electrolyte anion coordination as a general strategy to switch between reaction pathways, offering a new design principle for selective electrosynthetic transformations.

Received 1st February 2026

Accepted 8th May 2026

DOI: 10.1039/d6sc00891g

rsc.li/chemical-science

## Introduction

Electrochemical oxidation offers a sustainable and tunable platform for organic synthesis by enabling access to high-energy intermediates without the use of stoichiometric oxidants.<sup>1–3</sup> Among these intermediates, aromatic radical cations generated *via* single-electron transfer are particularly attractive because of their pronounced electrophilicity and unique reaction pathways.<sup>4–11</sup> However, controlling the reactivity of  $\pi$ -delocalized radical cations remains a fundamental challenge: once formed, these open-shell species often undergo indiscriminate follow-up reactions or persist without productive bond formation, thereby limiting synthetic selectivity (Fig. 1A).

To date, strategies to regulate electrochemical reactivity have largely focused on electrode materials, electrical potential, and solvent effects.<sup>12–14</sup> In contrast, supporting electrolytes are most often treated as passive components that merely ensure ionic conduction and charge balance. However, this conventional view has long been known to be incomplete. Classical studies in aromatic electrochemistry have shown that electrolyte identity

and ion-pairing can influence redox potentials, electron-transfer kinetics, and product distributions.<sup>15–17</sup> More recent discussions have further emphasized that supporting electrolytes can play roles beyond conductivity.<sup>18–22</sup>

Despite these important precedents, systematic experimental demonstrations of how electrolyte anions switch the fate

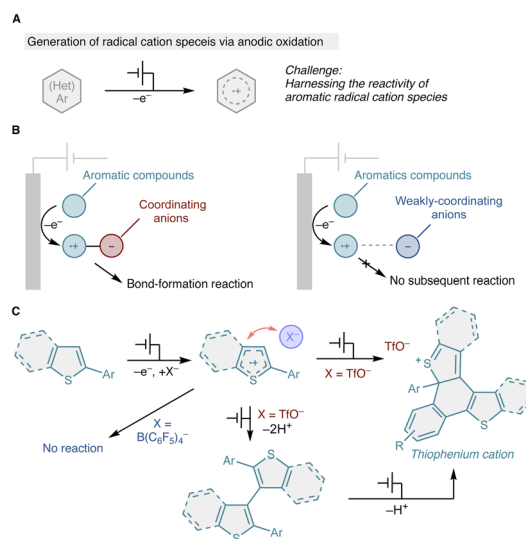


Fig. 1 Conceptual overview of this work. (A) Reactivity control of aromatic radical cations. (B) Electrolyte-anion-controlled switching of radical cation reactivity. (C) Oxidative C–C bond formation and cyclization of diarylthiophene derivatives.

<sup>a</sup>Department of Chemistry and Life Science, Yokohama National University, 79-5 Tokiwadai, Hodogaya-ku, Yokohama 240-8501, Japan. E-mail: shida-naoki-gz@ynu.ac.jp; atobe-mahito-wk@ynu.ac.jp

<sup>b</sup>Institute of Advanced Sciences, Yokohama National University, 79-5 Tokiwadai, Hodogaya-ku, Yokohama 240-8501, Japan

<sup>c</sup>PRESTO, Japan Science and Technology Agency (JST), 4-1-8 Honcho, Kawaguchi, Saitama 332-0012, Japan

<sup>d</sup>Department of Chemical Science and Engineering, School of Materials and Chemical Technology, Institute of Science Tokyo, Nagatsuta-cho 4259, Midori-ku, Yokohama 226-8501, Japan. E-mail: inagi@mct.isct.ac.jp

of electrogenerated aromatic radical cations between persistence and productive bond formation remain limited. In particular, direct comparison of weakly coordinating and more strongly coordinating anions within a defined substrate class, combined with spectroscopic observation of radical-cation accumulation and preparative validation of downstream C–C bond formation, has not been fully established.

Building on these precedents, we asked whether electrolyte-anion effects could be translated into a more deliberate strategy for controlling the lifetime and follow-up reactivity of aromatic radical cations (Fig. 1B). Specifically, a coordinating anion may engage an electrogenerated aromatic radical cation through specific anion association, perturbing its electronic structure and lowering the kinetic barrier for productive bond-forming pathways. Conversely, weakly coordinating anions<sup>23</sup> may stabilize the radical cation state, favoring its persistence over follow-up chemistry.

Herein, we demonstrate that electrolyte anion coordination decisively governs the reactivity of radical cations generated from  $\pi$ -extended thiophene derivatives. Using triflate ( $\text{TfO}^-$ ) as a coordinating anion, anodic oxidation selectively promotes C–C bond formation, leading to dimerization and subsequent oxidative cyclization to form thiophenium cations *via* an overall two-electron process (Fig. 1C). In contrast, weakly coordinating anions ( $\text{B}(\text{C}_6\text{F}_5)_4^-$ ) stabilize persistent and largely unreactive radical cations. These findings establish electrolyte anion coordination as a general strategy to modulate radical cation reactivity and selectively access bond-forming pathways in organic electrosynthesis.

## Results and discussion

Cyclic voltammetry (CV) of 2,5-diphenylthiophene (**PTh-H**) was first examined in dichloromethane (Gutman's donor number:  $\text{CH}_2\text{Cl}_2 = 1$ )<sup>24</sup> using a series of tetrabutylammonium salts with counter anions of varying donor strength (Fig. 2A).<sup>25</sup> When weakly coordinating anions such as  $\text{B}(\text{C}_6\text{F}_5)_4^-$  and  $\text{PF}_6^-$  were employed, **PTh-H** exhibited a fully reversible one-electron oxidation. In contrast, progressively less reversible behavior was observed with increasing anion donor number, and in the presence of the strongly coordinating triflate anion ( $\text{TfO}^-$ ), the oxidation became completely irreversible and was accompanied by a pronounced increase in anodic current. These results indicate that the electrochemical behavior of **PTh-H** is highly sensitive to the identity of the supporting electrolyte anion.

The influence of anion coordination was further confirmed by incremental addition of  $\text{Bu}_4\text{NTfO}$  to a solution of **PTh-H** in a weakly coordinating electrolyte ( $\text{Bu}_4\text{NPF}_6/\text{CH}_2\text{Cl}_2$ ). Even small amounts of  $\text{TfO}^-$  markedly transformed the voltammetric response from a reversible one-electron process to an irreversible oxidation with enhanced current (Fig. 2A, right), demonstrating that  $\text{TfO}^-$  directly perturbs the fate of the oxidized species rather than acting as a passive spectator.

To identify the electrochemically generated intermediates, spectroelectrochemical measurements were performed (Fig. 2B). In the presence of the weakly coordinating  $\text{B}(\text{C}_6\text{F}_5)_4^-$  anion, oxidation of **PTh-H** produced characteristic absorption

bands at 770 and 490 nm, which are assigned to the HOMO–SOMO and SOMO–LUMO transitions of the radical cation **PTh-H**<sup>•+</sup>.<sup>20</sup> By contrast, oxidation in the presence of  $\text{TfO}^-$  resulted in a distinct spectral profile with absorption maxima at 690 and 430 nm, indicating the formation of a different cationic species. These observations suggest that although initial electron transfer occurs under both conditions, the subsequent chemical fate of the oxidized intermediate is strongly dependent on anion coordination.

Bulk electrolysis experiments provided decisive insight into this divergence (Fig. 2C). Electrolysis of **PTh-H** under weakly coordinating conditions ( $\text{Bu}_4\text{NB}(\text{C}_6\text{F}_5)_4/\text{CH}_2\text{Cl}_2$ ) with passage of  $1 \text{ F mol}^{-1}$  of charge yielded a purple solution whose UV-vis and EPR spectra were fully consistent with the persistent radical cation **PTh-H**<sup>•+</sup>. In contrast, electrolysis under coordinating conditions ( $\text{Bu}_4\text{NTfO}/\text{CH}_2\text{Cl}_2$ ) afforded a green solution that was EPR silent despite the same charge being passed. <sup>1</sup>H NMR analysis revealed the presence of both unreacted **PTh-H** and a new dimeric species, identified as the thiophenium salt  $[(\text{PTh-H})_2][\text{TfO}]$ . Notably, formation of this product formally requires a two-electron oxidation per **PTh-H** unit, indicating that successive oxidation is favored over accumulation of the radical cation in the presence of  $\text{TfO}^-$ .

Consistent with this interpretation, electrolysis under coordinating conditions with passage of  $2 \text{ F mol}^{-1}$  of charge resulted in clean and quantitative formation of  $[(\text{PTh-H})_2][\text{TfO}]$  as the sole detectable species (Fig. 2D). The structure of the thiophenium salt was established by multinuclear NMR and mass spectroscopy (see SI). These results demonstrate that coordination of  $\text{TfO}^-$  modulates the intrinsic reactivity of the radical cation generated by one-electron oxidation of **PTh-H**, thereby enabling subsequent bond-forming reactions that lead to an overall two-electron transformation.

This anion-controlled transformation was also observed for a series of related substrates (Fig. 2D). Electrochemical oxidation of symmetrical biarylthiophenes bearing <sup>-1</sup>Pr or <sup>-</sup>CF<sub>3</sub> substituents at the *para*-position of the aryl groups (**PTh-<sup>-1</sup>Pr**, and **PTh-CF<sub>3</sub>**) under coordinating conditions led to clean formation of the corresponding thiophenium salts.

To unambiguously establish the structure of thiophenium salts, a subsequent chemical transformation was carried out using  $[(\text{PTh-CF}_3)_2][\text{TfO}]$  (Fig. 2D). Upon addition of *N,N*-dimethylaniline to the electrochemically generated  $[(\text{PTh-CF}_3)_2][\text{TfO}]$  without purification, the characteristic green coloration disappeared immediately. The product obtained in 80% yield was subjected to single-crystal X-ray diffraction analysis, which confirmed the formation of compound **1**, a Pummerer-type reaction product. Since Pummerer reactions are characteristic transformations of thiophenium and thionium salts,<sup>26–28</sup> this result provides compelling evidence that  $[(\text{PTh-CF}_3)_2][\text{TfO}]$  indeed possesses the expected thiophenium-type structure.

To probe whether anion coordination also influences the subsequent cyclization step, the independently synthesized dimeric precursor **bis(PTh-H)** was subjected to electrochemical oxidation (Fig. 2E). In the presence of  $\text{TfO}^-$ , **bis(PTh-H)** underwent irreversible oxidation to afford the corresponding thiophenium cation, consistent with a coordination-assisted



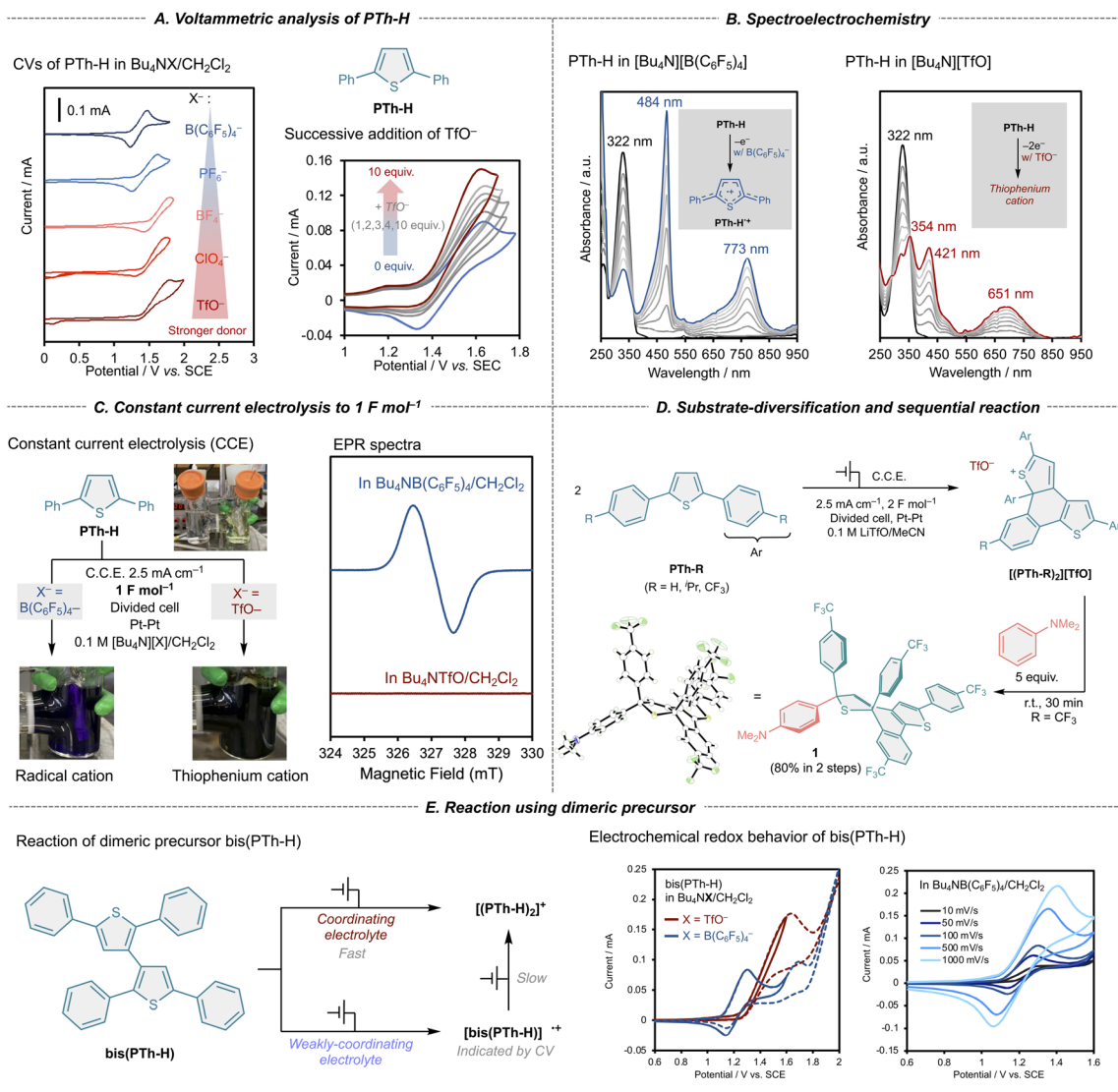


Fig. 2 Electrochemical behaviour of PTh-H in the presence of coordinating and weakly coordinating anions. (A) Cyclic voltammograms of PTh-H in  $\text{CH}_2\text{Cl}_2$  containing various supporting electrolytes. (B) UV-vis spectroelectrochemical spectra recorded under anodic oxidation. (C) Bulk electrolysis and EPR analysis under weakly coordinating and coordinating conditions. (D) Substrate diversification of PTh-R and subsequent transformation. (E) Electrochemical oxidation of independently synthesised bis(PTH-H).

two-electron process. In contrast, oxidation in the presence of the weakly coordinating  $\text{B}(\text{C}_6\text{F}_5)_4^-$  anion exhibited partially reversible behavior, with scan-rate-dependent irreversibility becoming more pronounced at slower scan rates (Fig. 2E). These observations suggest that anion coordination not only governs the initial oxidation state of PTh-H but also facilitates the oxidative cyclization of the dimeric intermediate.

Taken together, the combined electrochemical, spectroscopic, and bulk electrolysis data establish that specific association of  $\text{TfO}^-$  fundamentally alters the reaction pathway of electrogenerated PTh-H<sup>+</sup>, selectively promoting C-C bond formation *via* an overall two-electron oxidation process.

To further elucidate the role of anion coordination in the intermolecular C-C bond-forming step, we next investigated the electrochemical oxidation of benzo[*b*]thiophene derivative,

BTh, as a mechanistically simpler model system (Fig. 3). Unlike PTh-H, BTh undergoes selective intermolecular dimerization prior to cyclization, allowing direct interrogation of the C-C coupling process. Under weakly coordinating conditions, anodic oxidation of BTh generated the corresponding radical cation BTh<sup>•+</sup>, as confirmed by spectroscopic analysis, but no productive bond formation was observed. In contrast, electrolysis in the presence of the coordinating  $\text{TfO}^-$  anion resulted in efficient formation of the 3,3'-dimer bis(BTh) upon passage of 1 F mol<sup>-1</sup> of charge (Fig. 3A). When 2 F mol<sup>-1</sup> of charge was passed under otherwise identical conditions, the corresponding thiophenium salt [(BTh)<sub>2</sub>][TfO] was obtained selectively. These results indicate that, for BTh, intermolecular dimerization precedes oxidative cyclization, in contrast to the partially overlapping processes observed for PTh-H.



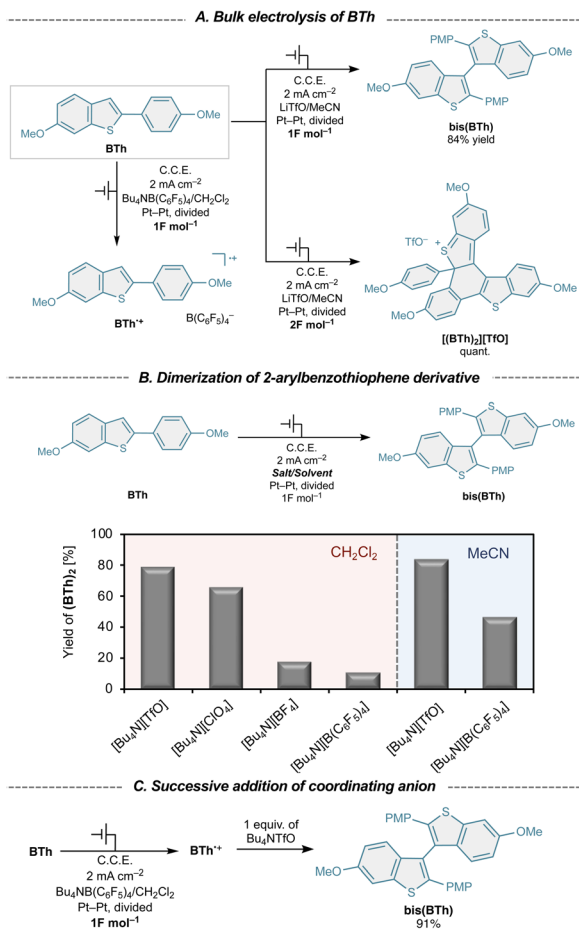


Fig. 3 Electrochemical oxidation of BTh under coordinating and weakly coordinating conditions. (A) Bulk electrolysis of BTh in  $\text{CH}_2\text{Cl}_2$  using different supporting electrolytes. (B) Yield of  $\text{bis}(\text{BTh})$  as a function of the electrolyte anion. (C) Electrochemical generation of  $\text{BTh}^{\bullet+}$  under weakly coordinating conditions, followed by post-electrolysis addition of a coordinating anion.

The effect of electrolyte anion identity on the dimerization step was systematically examined (Fig. 3B). Electrolysis of  $\text{BTh}$  ( $1 \text{ F mol}^{-1}$ ) in dichloromethane revealed a strong dependence

of dimer yield on anion donor strength, with  $\text{TfO}^-$  providing the highest efficiency. In sharp contrast, the weakly coordinating  $\text{B}(\text{C}_6\text{F}_5)_4^-$  anion predominantly stabilized the radical cation, suppressing C–C bond formation. These observations indicate that anion coordination is a critical factor in enabling productive intermolecular coupling of  $\text{BTh}$  radical cations. Solvent effects further support this conclusion. When acetonitrile, a coordinating solvent (Gutman's donor number:  $\text{MeCN} = 14.1$ ),<sup>24</sup> was employed, dimerization occurred even in the presence of  $\text{B}(\text{C}_6\text{F}_5)_4^-$ , although the yield remained significantly higher with  $\text{TfO}^-$ . This behavior suggests that coordination plays a decisive role in promoting C–C bond formation from radical cation intermediates.

To directly probe whether  $\text{TfO}^-$  interacts with the radical cation during the coupling step, a cation-pool approach was employed.<sup>29</sup>  $\text{BTh}^{\bullet+}$  was first generated electrochemically under weakly coordinating conditions by passage of  $1 \text{ F mol}^{-1}$  of charge, after which electrolysis was halted and  $\text{Bu}_4\text{NTfO}$  was added (Fig. 3C). Remarkably, this post-electrolysis addition of  $\text{TfO}^-$  resulted in rapid and near-quantitative formation of  $\text{bis}(\text{BTh})$  (91% yield). This experiment clearly demonstrates that  $\text{TfO}^-$  engages with  $\text{BTh}^{\bullet+}$  after electron transfer, actively facilitating intermolecular C–C bond formation rather than merely influencing the initial oxidation event.

Importantly, the quantitative formation of  $\text{bis}(\text{BTh})$  upon passage of exactly  $1 \text{ F mol}^{-1}$  of charge establishes that dimerization proceeds through an EC mechanism involving coupling of two radical cations, rather than an ECEC pathway. Taken together, the  $\text{BTh}$  system provides compelling evidence that coordinating anions act catalytically to unlock otherwise inaccessible radical cation coupling pathways, reinforcing the generality of anion-controlled switching of radical cation intermediates.

On the basis of the experimental observations described above, we propose a mechanism in which coordination of a supporting electrolyte anion modulates the intrinsic reactivity of electrogenerated radical cations (Fig. 4). Under weakly coordinating conditions, anodic oxidation of  $\text{PTh-R}$  proceeds *via* a clean one-electron process to generate the corresponding radical cation. Owing to the  $\pi$ -extended framework of the

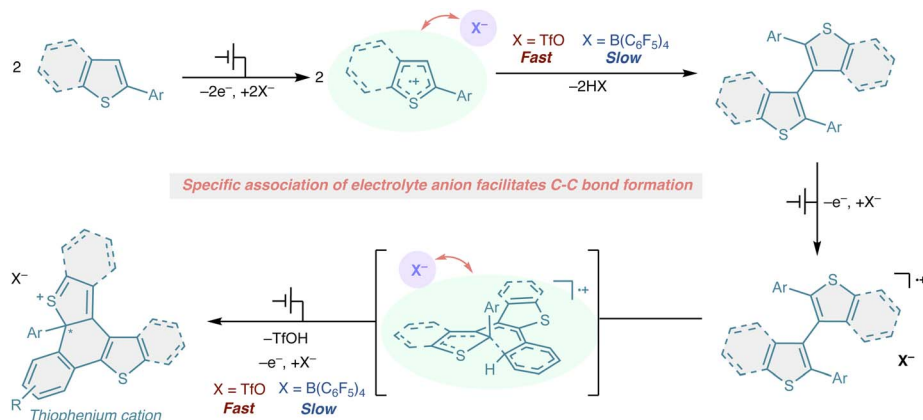


Fig. 4 Plausible reaction mechanism.



diarylthiophene scaffold, this radical cation is sufficiently stabilized to persist without engaging in productive follow-up reactions. In the presence of a coordinating anion such as  $\text{TfO}^-$ , the initial electron-transfer step similarly generates a radical cation. However, specific association of  $\text{TfO}^-$  to this open-shell intermediate perturbs its electronic structure, destabilizing the nonreactive radical cation state and rendering it susceptible to C–C bond-forming reactions. As a consequence, radical cation–radical cation coupling becomes kinetically accessible, leading to intermolecular C–C bond formation. Importantly, the effect of  $\text{TfO}^-$  coordination is not limited to intermolecular coupling. The same anion-induced activation also accelerates the subsequent intramolecular oxidative cyclization of the dimeric intermediate. In this context,  $\text{TfO}^-$  does not act as a stoichiometric reagent but rather as a promoter that facilitates both inter- and intramolecular C–C bond formation from radical cation intermediates. It should be noted that the role of  $\text{TfO}^-$  in this process may not be limited to modulation of the radical-cation state through coordination. Because C–C bond formation is accompanied by deprotonation,  $\text{TfO}^-$  may also assist proton transfer as a local proton acceptor after association with the cationic radical manifold. Protons released during C–C bond formation and oxidative cyclization are expected to be transferred as proton equivalents through the non-aqueous electrolyte and eventually reduced at the cathode, most likely to form  $\text{H}_2$ .

Taken together, these findings suggest that coordinating anions such as  $\text{TfO}^-$  function as catalysts in radical cation chemistry, modulating the reactivity landscape of open-shell intermediates and enabling bond-forming pathways that are otherwise disfavored under electrochemical conditions.

## Conclusions

In conclusion, we have demonstrated that coordination of supporting electrolyte anions provides a powerful means to regulate the reactivity of electrogenerated radical cations. Using 2,5-diarylthiophenes as a model system, we showed that weakly coordinating anions stabilize persistent radical cations, whereas specific association of triflate ( $\text{TfO}^-$ ) electronically activates these open-shell intermediates, enabling both intermolecular C–C coupling and subsequent intramolecular oxidative cyclization.

Importantly, the role of the coordinating anion is not to directly induce a second electron-transfer event but to modulate the intrinsic reactivity of radical cations, rendering otherwise disfavored bond-forming pathways kinetically accessible under electrochemical conditions. In this context, the electrolyte anion functions in a catalytic manner, controlling the reaction landscape without being consumed.

More broadly, this work establishes electrolyte design as a general and conceptually simple approach to controlling radical cation reactivity in organic electrosynthesis. We anticipate that this principle will be broadly applicable to other classes of organic redox transformations, providing new opportunities for selective bond formation under electrochemical conditions.

## Author contributions

N. S., M. A., and S. I. coordinated the project. N. S., M. A., and S. I. conceived the project, designed the experiments, and wrote the manuscript. T. M. and Y. Y. carried out the synthetic experiments. S.-G. C. supported analysis and characterization. N. S., I. T., M. A., and S. I. contributed to discussing of the reaction mechanism and analysis of synthetic results.

## Conflicts of interest

There are no conflicts to declare.

## Data availability

The data presented in this study are available upon reasonable request from the corresponding authors.

CCDC 2526613 contains the supplementary crystallographic data for this paper.<sup>30</sup>

Supplementary information: all experimental procedures and characterisation data of all synthesized compounds. See DOI: <https://doi.org/10.1039/d6sc00891g>.

## Acknowledgements

This work was financially supported by JSPS KAKENHI Grant Numbers 21H05215 (Digi-TOS), 23H04914 and 23H04916 (both from Green Catalysis Science), 23K23386, 23K17370. This work was supported by Japan Science and Technology Agency (JST) as part of Adopting Sustainable Partnerships for Innovative Research Ecosystem (ASPIRE), Grant Number JPMJAP2528. HRMS, scXRD, and NMR measurements were performed at the Instrumental Analysis Center at YNU and Core Facility Center at Science Tokyo.

## Notes and references

- 1 A. Wiebe, T. Gieshoff, S. Möhle, E. Rodrigo, M. Zirbes and S. R. Waldvogel, *Angew. Chem., Int. Ed.*, 2018, **57**, 5594–5619.
- 2 C. Zhu, N. W. J. Ang, T. H. Meyer, Y. Qiu and L. Ackermann, *ACS Cent. Sci.*, 2021, **7**, 415–431.
- 3 M. C. Leech, A. D. Garcia, A. Petti, A. P. Dobbs and K. Lam, *React. Chem. Eng.*, 2020, **5**, 977–990.
- 4 N. L. Bauld, *Tetrahedron*, 1989, **45**, 5307–5363.
- 5 A. Gieseler, E. Steckhan, O. Wiest and F. Knoch, *J. Org. Chem.*, 1991, **56**, 1405–1411.
- 6 K. Chiba, T. Miura, S. Kim, Y. Kitano and M. Tada, *J. Am. Chem. Soc.*, 2001, **123**, 11314–11315.
- 7 T. Miura, S. Kim, Y. Kitano, M. Tada and K. Chiba, *Angew. Chem., Int. Ed.*, 2006, **45**, 1461–1463.
- 8 S. P. Pitre, J. C. Scaiano and T. P. Yoon, *ACS Catal.*, 2017, **7**, 6440–6444.
- 9 S. M. Stevenson, M. P. Shores and E. M. Ferreira, *Angew. Chem., Int. Ed.*, 2015, **54**, 6506–6510.
- 10 R. Nagaya, T. Seko, K. Okamoto, K. Ueno, M. Atobe and N. Shida, *Nat. Commun.*, 2025, **16**, 10679.



- 11 K. Rybicka-Jasińska, Z. Szeptuch, H. Kubiszewski and A. Kowaluk, *Org. Lett.*, 2023, **25**, 1142–1146.
- 12 D. S. P. Cardoso, B. Šljukić, D. M. F. Santos and C. A. C. Sequeira, *Org. Process Res. Dev.*, 2017, **21**, 1213–1226.
- 13 M. C. Leech and K. Lam, *Nat. Rev. Chem.*, 2022, **6**, 275–286.
- 14 M. Brachi, W. El Housseini, K. Beaver, R. Jadhav, A. Dantanarayana, D. G. Boucher and S. D. Minter, *ACS Org. Inorg. Au*, 2024, **4**, 141–187.
- 15 N. L. Weinberg and T. B. Reddy, *J. Am. Chem. Soc.*, 1968, **90**, 91–94.
- 16 M. K. Kalinowski, *Chem. Phys. Lett.*, 1971, **8**, 378–380.
- 17 J.-M. Savéant, *J. Phys. Chem. B*, 2001, **105**, 8995–9001.
- 18 B. B. Noble, P. L. Norcott, C. L. Hammill, S. Ciampi and M. L. Coote, *J. Phys. Chem. C*, 2019, **123**, 10300–10305.
- 19 N. Shida, Y. Imada, S. Nagahara, Y. Okada and K. Chiba, *Commun. Chem.*, 2019, **2**, 3–5.
- 20 N. Shida, H. Nishiyama, F. Zheng, S. Ye, D. S. Seferos, I. Tomita and S. Inagi, *Commun. Chem.*, 2019, **2**, 124.
- 21 N. Shida, *Electrochemistry*, 2022, **90**, 101004.
- 22 L. G. Gombos, J. Nikl and S. R. Waldvogel, *ChemElectroChem*, 2024, **11**, e202300730.
- 23 S. H. Strauss, *Chem. Rev.*, 1993, **93**, 927–942.
- 24 F. Cataldo, *Eur. Chem. Bull.*, 2015, **4**, 92–97.
- 25 M. Schmeisser, P. Illner, R. Puchta, A. Zahl and R. Van Eldik, *Chem.–Eur. J.*, 2012, **18**, 10969–10982.
- 26 S. K. Bur and A. Padwa, *Chem. Rev.*, 2004, **104**, 2401–2432.
- 27 K. S. Feldman, *Tetrahedron*, 2006, **62**, 5003–5034.
- 28 S. Akai and Y. Kita, in *Sulfur-Mediated Rearrangements I*, Springer Berlin Heidelberg, Berlin, Heidelberg, 2006, pp. 35–76.
- 29 J.-I. I. Yoshida, A. Shimizu and R. Hayashi, *Chem. Rev.*, 2018, **118**, 4702–4730.
- 30 CCDC 2526613: Experimental Crystal Structure Determination, 2026, DOI: [10.5517/ccdc.csd.cc2qt4nc](https://doi.org/10.5517/ccdc.csd.cc2qt4nc).

